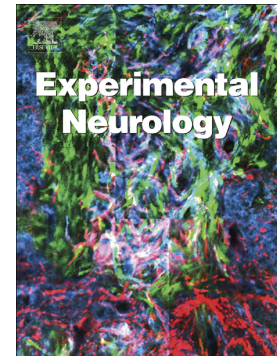# Accepted Manuscript

Expression of pathogenic SCN9A mutations in the zebrafish: A model to study small fiber neuropathy

Ivo Eijkenboom, Maurice Sopacua, Auke B.C. Otten, Monique M. Gerrits, Janneke G.J. Hoeijmakers, Stephen G. Waxman, Raffaella Lombardi, Giuseppe Lauria, Ingemar S.J. Merkies, Hubert J.M. Smeets, Catharina G. Faber, Jo M. Vanoevelen, on behalf of the PROPANE Study Group

Please cite this article as: Ivo Eijkenboom, Maurice Sopacua, Auke B.C. Otten, Monique M. Gerrits, Janneke G.J. Hoeijmakers, Stephen G. Waxman, Raffaella Lombardi, Giuseppe Lauria, Ingemar S.J. Merkies, Hubert J.M. Smeets, Catharina G. Faber, Jo M. Vanoevelen, on behalf of the PROPANE Study Group , Expression of pathogenic SCN9A mutations in the zebrafish: A model to study small fiber neuropathy. Yexnr (2018), doi:10.1016/j.expneurol.2018.10.008

Expression of pathogenic *SCN9A* mutations in the zebrafish: a model to study small fiber neuropathy

Ivo Eijkenboom[a,b], Maurice Sopacua[b,c], Auke B.C. Otten[a], Monique M. Gerrits[d], Janneke G.J. Hoeijmakers[b,c], Stephen G. Waxman[e], Raffaella Lombardi[f], Giuseppe Lauria[f,g], Ingemar S.J. Merkies[c,h], Hubert J.M. Smeets[a], Catharina G. Faber[b,c], Jo M. Vanoevelen[d,i] on behalf of the PROPANE Study Group*

[a]Department of Genetics and Cell Biology, Clinical Genomics Unit, Maastricht University, Maastricht, The Netherlands.

[b]MHeNs school for Mental Health and Neuroscience, Maastricht University, Maastricht, The Netherlands.

[c]Department of Neurology, Maastricht University Medical Center+, Maastricht, The Netherlands.

[d]Department of Clinical Genetics, Maastricht University Medical Center+, Maastricht, The Netherlands.

[e]Center for Neuroscience and Regeneration Research, VA Connecticut Healthcare System, West Haven, USA.

[f]Neuroalgology Unit, IRCCS Fondazione Istituto Neurologico "Carlo Besta", Milan, Italy

[g]Department of Biomedical and Clinical Sciences "Luigi Sacco", University of Milan, Milan, Italy.

[h]Department of Neurology, St. Elisabeth Hospital, Willemstad, Curaçao.

[i]GROW-School for Oncology and Developmental Biology, Maastricht University, Maastricht, The Netherlands.

Corresponding author:

Catharina G. Faber, MD, PhD

Department of Neurology

Maastricht University Medical Center+

P.O. Box 5800

6202 AZ Maastricht, The Netherlands

T: +31 43 3877059

F: +31 43 3877055

E-mail: c.faber@mumc.nl

*PROPANE Study Group:

de Greef B, Lindsey P, Al Momani R, Yang Y, Taiana M, Marchi M, Cazzato D, Boneschi FM, Zauli A, Clarelli F, Santoro S, Lopez I, Quattrini A, Cestèle S, Chever O, Tavakoli M, Mailk R, Ziegler D, Kapetis D, Xenakis MN, Westra R, Szklarczyk R, Mantegazza M

Keywords: Small fiber neuropathy, *SCN9A* mutations, zebrafish model, nerve density, temperature assay.

Abstract

Small fiber neuropathy (SFN) patients experience a spectrum of sensory abnormalities, including attenuated responses to non-noxious temperatures in combination with a decreased density of the small-nerve fibers. Gain-of-function mutations in the voltage-gated sodium channels *SCN9A*, *SCN10A* and *SCN11A* have been identified as an underlying genetic cause in a subpopulation of patients with SFN. Based on clinical-diagnostic tests for SFN, we have set up a panel of two read-outs reflecting SFN in zebrafish, being nerve density and behavioral responses. Nerve density was studied using a transgenic line in which the sensory neurons are GFP-labelled. For the behavioral experiments, a temperature-controlled water compartment was developed. This device allowed quantification of the behavioral response to temperature changes. By using these read-outs we demonstrated that zebrafish embryos transiently overexpressing the pathogenic human *SCN9A* p.(I228M) or p.(G856D) mutations both have a significantly decreased density of the small-nerve fibers. Additionally, larvae overexpressing the p.(I228M) mutation displayed a significant increase in activity induced by temperature change. As these features closely resemble the clinical hallmarks of SFN, our data suggest that transient overexpression of mutant human mRNA provides a model for SFN in zebrafish. This disease model may provide a basis for testing the pathogenicity of novel genetic variants identified in SFN patients. Furthermore, this model could be used for studying SFN pathophysiology in an *in vivo* model and for testing therapeutic interventions.

Introduction

Patients with small fiber neuropathy (SFN) typically complain of length-dependent neuropathic pain symptoms due to dysfunction and degeneration of thinly-myelinated Aδ and unmyelinated C-fibers (Hoeijmakers et al., 2012a, Cazzato and Lauria, 2017). Pain symptoms can be spontaneous (e.g. burning, deep, paroxysmal pain) and evoked by innocuous stimuli (e.g. light touch or pressure, warm and cold water). The diagnosis of SFN is based on the characteristic clinical picture, and abnormal temperature threshold testing and/or reduced intraepidermal nerve fiber density (IENFD) in a skin biopsy (Cazzato and Lauria, 2017, Tesfaye et al., 2010, Hoeijmakers et al., 2012a). The spectrum of etiologies causing SFN has widened and includes gain-of-function (GOF) mutations in *SCN9A*, *SCN10A* and *SCN11A*, genes encoding Nav1.7, Nav1.8, and Nav1.9 alpha subunits of voltage-gated sodium channels, respectively (Cazzato and Lauria, 2017, Faber et al., 2012a, Han et al., 2015, Faber et al., 2012b). Conversely, patients with homozygous loss-of-function (LOF) mutations in *SCN9A* present with congenital indifference to pain (Cox et al., 2010). $Na_v1.7$, $Na_v1.8$, and $Na_v1.9$ are abundantly expressed in peripheral sensory neurons and their axons, where they play a pivotal role in the generation and conduction of action potentials (Ho and O'Leary, 2011, Black et al., 2012, Shields et al., 2012). All three belong to the same family of voltage-gated sodium channels, consisting of four functional domains with six transmembrane segments (S1-S6) (Wood and Baker, 2001, Marban et al., 1998).

Recently, a study in the Netherlands consisting of 921 patients diagnosed with SFN has revealed a prevalence of 16.7% of potentially pathogenic variants in one of these three sodium channel genes (de Greef et al., 2017). The pathogenicity of genetic variants in these human sodium channels could be demonstrated by segregation analysis in large families, when possible, or cell electrophysiological studies, which are expensive and time-consuming (Waxman et al., 2014). The characterization of these gene variants could also support the identification of new compounds targeting these sodium channels (Hoeijmakers et al., 2012a). The availability of a simple and rapid sodium channel gene-related *in vivo* model of SFN would provide a medium-throughput screening tool for testing novel genetic variants and allow testing the efficacy of available and new candidate analgesics. The zebrafish has proven to be an excellent model for neurological diseases and because of the many similarities between zebrafish and mammal neuroanatomical organization, it is a good candidate for modeling SFN (Malafoglia et al., 2013, Becker and Rinkwitz, 2012). The sensory

nervous system in zebrafish consists, like in mammals, of trigeminal ganglia, vagal ganglia and dorsal root ganglia (DRG) (Malafoglia et al., 2013). In addition, zebrafish have an early type of sensory neurons, Rohon Beard (RB) neurons, which allow the externally developing embryo to acquire sensory input leading to activation of escape behavior in case of environmental threats (Reyes et al., 2004, Malafoglia et al., 2013). Furthermore, the family of voltage-gated sodium channels in teleost species share high levels of identity with their mammalian counterparts and since s*cn1aa, scn8aa and scn8ab* are broadly expressed in the sensory nervous system, it is likely that sodium channels play an important role in nociception (Novak et al., 2006). Knockdown of *scn8aa* revealed a significant effect on inward sodium current in sensory neurons resulting in a reduced touch response, which was not observed in *scn1aa* morphants (Pineda et al., 2005). Zebrafish have been already used in nociception studies (Taylor et al., 2017, Prober et al., 2008) taking advantage of their escape behavior in response to noxious compounds and elevated water temperatures characterized by increased swimming activity (Gau et al., 2013, Prober et al., 2008, Curtright et al., 2015). Based on these observations, temperature aversion assays have been developed to test the potential analgesic properties of novel compounds (Curtright et al., 2015).

Here, we describe two read-outs for measuring SFN in zebrafish. These read-outs are based on two clinical hallmarks of SFN, that are the abnormal response to thermal stimuli (thermal allodynia) and the reduced density of sensory neurites. We tested the behavioral read-out by using a *scn8aa* LOF line which is expected to have an attenuated response to temperature change. To model SFN in the zebrafish, we have opted for the overexpression of human variants because the functional zebrafish ortholog of *SCN9A* has not been identified and mutations in this gene are inherited in an autosomal dominant manner. We overexpressed two human pathogenic *SCN9A* p.(I228M) and p.(G856D) GOF mutations that are causative of SFN (Persson et al., 2013, Hoeijmakers et al., 2012b, Estacion et al., 2011, Faber et al., 2012a).

Material & Methods

Zebrafish husbandry

Zebrafish (*Danio reiro*) were housed and raised in the zebrafish facility at Maastricht University. Briefly, zebrafish were maintained at a 14 hour light and 10 hour dark cycle, the water temperature was kept at 27°C and adults were fed twice a day (Avdesh et al., 2012). To obtain eggs, the day before mating males and females, separated by a divider, were placed in a breeding tank. The next day, after the lights were turned on, the divider was removed to allow mating. Eggs were collected and transferred to petri dishes containing E3 medium (Nusslein-Volhard and Dahm, 2002). The zebrafish line *sensory:GFP* used in this study was developed and described by O'Brien and coworkers (O'Brien et al., 2012). For all imaging studies, to avoid interference of pigmentation with the fluorescent signal, a *sensory:GFP* line in a nacre background was used lacking melanophores (Lister et al., 1999). The *scn8aa* LOF nebula zebrafish line tW1752X harbors a premature translation termination substitution and causes in a homozygous state a LOF of *scn8aa* (Wright et al., 2010). Genotyping was performed by KASP by design (LGC Genomics, Berlin, Germany) with a custom primer targeted to the following region:

5'CCGCTACAAGTGTTGCGATGTGCCCATCACGGAAGGCTGGGGCAAGAATT**[G/A]**GTGGTTTCTCCGAAAGACCTGCTAT CTGATTGTGGAGCACAACTGGTTTG3'

SCN9A **mRNA overexpression experiments**

Vectors containing wildtype *SCN9A* and mutant human *SCN9A* with GOF mutations (I228M/G856D) were kindly provided by S. G. Waxman and S. D. Dib-Hajj and were subcloned in a PCS2+ vector for *in vitro* mRNA synthesis (Estacion et al., 2011, Hoeijmakers et al., 2012b). To transcribe full-length mRNA the Ambion mMessage mMachine SP6 transcription kit (Invitrogen, Carlsbad, CA, USA) was used. mRNA quality was determined by denaturing RNA gel electrophoresis and quantity was assessed using the Qubit fluorometer 4 (Thermo Fischer Scientific, Waltham, MA, USA). A dose of 100pg of WT or mutant *SCN9A* mRNA was injected in the 1-2-cell stage of embryos of *sensory:GFP* or wild-types (AB). Expression of these constructs was confirmed at 96 hpf by amplification of the 3' coding sequence. RNA extractions were performed according to standard procedures with TRizol Reagent (Thermo Fischer Scientific, Waltham, MA, USA) and for the cDNA transcription, the qScript cDNA Synthesis Kit was used (Quanta, Beverly, MA, USA).

5

Confocal imaging & quantification of nerve densities

Prior to imaging with a DMI 4000B microscope (Leica, Wetzlar, Germany) equipped with a TCS SPE confocal laser scanning module (Leica, Wetzlar, Germany), manually dechorionated 48 hpf nacre *sensory:GFP* embryos expressing human *SCN9A* (mutant) mRNA, were anesthetized using tricaine mesylate (Saint Louis, MO, USA) and were embedded in 2% low melting-point agarose. Image acquisition of the caudal fin, allowing reproducibility between embryos, was performed using confocal sections of 1.01µm. After noise reduction using the LAS X software (version 3.3), each confocal recording was loaded in ImageJ software (version 1.50i) and z-projections were converted to 8-bit images. After manually adjusting the threshold, nerve densities were quantified in the caudal fin using the ImageJ Particle Analyzer. For each image, the mean pixel value was quantified in five independent areas which were subsequently averaged.

TUNEL staining & quantification of Rohon Beard neuron death

Terminal deoxynucleotidyl transferase dUTP nick-end labeling (TUNEL) staining was combined with whole-mount immunocytochemistry as described previously (Svoboda et al., 2001). For the TUNEL staining, we used the *in situ* cell death detection kit, TMR red (Sigma Aldrich, Saint Louis, MO, USA). After the TUNEL staining nacre *sensory:GFP* embryos (48 hpf) expressing human *SCN9A* (mutant) mRNA were in a dorsal position embedded in 2% low melting-point agarose and imaged with a DMI 4000B microscope (Leica, Wetzlar, Germany) equipped with a TCS SPE confocal laser scanning module (Leica, Wetzlar, Germany). Image acquisition was performed using confocal sections of 4.15µm. After noise reduction using the LAS X software (version 3.3), each recording was loaded in ImageJ software (version 1.50i) and z-projections were blinded and the number of apoptotic RB neurons was counted manually.

ZebraBox experiments

Temperature sensitivity was assessed with an add-on, developed in-house, to the ZebraBox system (Viewpoint, Lyon, France and Maastricht Instruments BV., Maastricht, The Netherlands), consisting of 2 water reservoirs with water at a high temperature (50.0°C) and water at a baseline temperature (28.5°C) (fig.2). This setup enabled us to rapidly increase the

water temperature in the water compartment from 28.5°C ± 0.1°C to 41.0°C ± 0.7°C. The temperature inside the wells during baseline recording was 27.7 °C and the maximum temperature, reached at the end of the experiment, was 39.6 °C ± 0.5°C. At 96 hpf, zebrafish larvae in a 48-well plate containing 500μl E3 were placed in the water compartment. After an adaptation period of 30 minutes in the dark, at 28.5°C ± 0.1°C, the protocol started with a baseline recording for 10 minutes at 28.5°C ± 0.1°C, followed by an increase of the water temperature. Zebralab software (Viewpoint) determines the size of the zebrafish by contrast differences between zebrafish and background. The software records the movement of the zebrafish and determines the activity by the number of pixels that change from one frame to the next.

Statistical analysis

GraphPad Prism version 5.02 was used to carry out statistical analysis, including student *t*-tests and data were considered significant when the calculated p-value <0.05. All data are presented as an average ± standard error of the mean (SEM).

Results

Read-out panel based on clinical hallmarks of SFN

We used a *sensory:GFP* zebrafish line to quantify nerve density in zebrafish embryos. This line allowed visualization of all sensory neurons and enabled us to study the density of sensory neurites in zebrafish. Development of sensory neurites in the zebrafish caudal fin was monitored during the first stages of development (fig.1). At 48 hours post-fertilization (hpf), marked by the red frame, a fully developed network of sensory neurites was formed (fig. 1). Extension of this network was observed in the following stage (56 hpf fig.1). Since retraction of some neurites occurred at later stages (>48 hpf), all confocal recordings were performed at 48 hpf (Svoboda et al., 2001).

In the second read-out, we aimed at measuring the behavioral responses to increased water temperatures. Therefore, we developed an add-on to the commercially-available behavioral tracking device, the ZebraBox (fig. 2A,B). This add-on was developed in-house and allowed to rapidly increase the water temperature in the water compartment containing a 48-well plate with the zebrafish larvae (fig.2B). A more detailed description of this module is given in the supplemental material (Supp. fig. 1-3) To explore the dynamics of the temperature change, 6 test runs were performed without larvae (fig. 2C). Recording for 10 minutes at baseline temperature revealed minor temperature fluctuations in the water temperature in the compartment (28.5°C ± 0.1°C), however, the temperature inside was for all tests the same 27.7 °C ± 0.0°C. Furthermore, these pilot experiments demonstrated that we were able to rapidly increase the water temperature (fig. 2C). Since the water in the wells is indirectly heated by the water in the compartment, the temperature inside the wells is lower than the water temperature in the compartment (fig. 2C).

In order to test our temperature set-up, we used non-injected controls (Supp. fig. 4) and a *scn8aa* LOF model having a defect in the processing of sensory stimuli caused by a loss of an endogenous zebrafish sodium channel (Low et al., 2010, Wright et al., 2010). Nebula (*scn8aa LOF)* mutant zebrafish embryos were selected based on a reduced touch response at 48 hpf and divided into two groups; homozygous mutant embryos with a diminished touch response and heterozygous mutant and homozygous WT siblings with a normal touch

8

response (Pineda et al., 2005, Wright et al., 2010). At 96 hpf, these groups were transferred to the water compartment. After an adaptation period of 30 minutes and baseline recording at 27.7°C the larvae were exposed to the rapid temperature change with a maximum of 39.6°C ± 0.5°C. As reported before zebrafish larvae responded to the temperature change with an increase in swimming activity which further increased as the temperature rose (Prober et al., 2008) (fig.3). At all the elevated temperatures the *scn8aa* mutants displayed significantly decreased activity compared to the control siblings (fig.3). The difference in activity between mutants and controls became more prominent as the temperature increased further (fig.3). For both groups, the activity of larvae peaked during heating but then gradually declined (fig.3). All larvae survived the heating protocol and no defects or abnormalities were observed afterwards.

Decreased nerve density in zebrafish expressing mutant *SCN9A*

Since *SCN9A* GOF mutations are inherited in an autosomal dominant manner and the zebrafish ortholog of *SCN9A* is unknown, we overexpressed in zebrafish either WT human *SCN9A* or one of two known human pathogenic mutations in the *SCN9A* gene, p.(I228M) and p.(G856D) (Hoeijmakers et al., 2012b, Persson et al., 2013, Estacion et al., 2011, Faber et al., 2012a). No developmental or morphological differences were observed in the first 4 days of development in zebrafish embryos expressing (mutant) human *SCN9A* (Supp. fig. 5). Expression of the mutant and *SCN9A*-WT mRNA was confirmed by RT-PCR (Supp. fig. 6).

At 48 hpf, we observed a significantly decreased density of sensory neurites in the caudal fin of zebrafish embryos expressing the p.(I228M) substitution (20.9% ± 2.8% n= 13) and the p.(G856D) substitution (17.1% ± 4.6% n= 7) compared to embryos expressing the $Na_v1.7$ wildtype protein (SCN9-WT 33,3% ± 1.4 n= 12) (fig.4).

Increased temperature-related activity in zebrafish expressing mutant *SCN9A* protein

Next, we determined the behavioral response of larvae (96 hpf) with overexpressed human mutant or *SCN9A*-WT to the temperature change. As a result of the temperature elevation, both groups, mutant and *SCN9A*-WT injected embryos, responded with an increase of their activity (fig. 5A,C). At lower temperatures, no significant differences were observed in the activity of larvae expressing mutant or *SCN9A*-WT. However, at higher temperatures, timepoints 14 and 15 minutes, a significant increase in activity was observed for larvae

expressing the p.(I228M) mutation (fig. 5A,B). In contrast, for embryos expressing the p.(G856D) mutation, we observed no significant different response to the temperature change at all time points (fig.5C,D). As observed for the *scn8aa* mutants and control siblings, the activity of larvae declined gradually after reaching a maximum (fig.5A,C, and fig.3).

Discussion

A recent study performed by our group reported a frequency of 16.7% of potentially pathogenic genetic variants of *SCN9A, SCN10A* and *SCN11A* in an SFN patient cohort (de Greef et al., 2017). This group contains a high number of variants of unknown clinical significance (VUS). Since *in silico* prediction algorithms are not infallible, cell electrophysiology experiments are time-consuming and co-segregation analysis cannot provide definite evidence, there is the need for a model to provide functional data of these genetic variants (Waxman et al., 2014, Hoeijmakers, 2014). Furthermore, the model could allow investigating *in vivo* the efficacy of available and new candidate analgesics at preclinical level.

Here, we report a zebrafish model of SFN, based on overexpression of human mutant mRNA, providing a platform that may allow testing the pathogenicity of potentially pathogenic *SCN9A* variants identified in patients.

The read-outs used in our study were based on clinical hallmarks of SFN, such as thermal allodynia and loss of the intraepidermal nerve fiber density in a skin biopsy (IENFD) (Devigili et al., 2008, Cazzato and Lauria, 2017, Tesfaye et al., 2010, Hoeijmakers et al., 2012a). We included the quantification of sensory neuritis in a *sensory:GFP* zebrafish line and the behavioral analysis based on the assay of swimming activity in response to the increase of water temperature. It was performed developing a temperature-controlled water compartment that was used as an add-on to the ZebraBox. To assess whether we were able to reveal differences in responses to temperature changes, we used the *scn8aa* LOF model with a defect in sensory perception that recapitulates the picture of congenital indifference to pain of patients harboring LOF mutations of *SCN9A* (Cox et al., 2010, Pineda et al., 2005). Our assay showed a severely diminished reaction to elevated water temperatures of homozygous mutants. This difference became more apparent at higher temperatures, demonstrating that we were able to reveal behavioral differences in temperature response with our assay. Therefore, the presence of *scn8aa*, a key player in sodium influx, in the sensory nervous system and a LOF of *scn8aa* that significantly affects the response to noxious temperatures, suggest that *scn8aa* could be at least partially orthologous to *SCN9A*. Furthermore, these embryos do not manifest severe motor deficits and retain the capability to swim, demonstrated by the initial temperature response observed in our mutants.

11

Supporting these findings, fictive swimming could be induced in zebrafish with a LOF of *scn8aa* (Low et al., 2010).

To model SFN in the zebrafish we overexpressed two pathogenic human mutations in *SCN9A,* p.(I228M) and p.(G856D) that are known to be causative of SFN in patients. Voltage and current clamp studies revealed that these mutations modulate sensory neuron functioning (Estacion et al., 2011, Hoeijmakers et al., 2012b, Faber et al., 2012a). Our experiments revealed that embryos expressing the p.(I228M) or the p.(G856D) mutation have a significantly decreased density of sensory neurites in the caudal fin. These findings in zebrafish paralleled the observations in SFN patients, harboring these mutations, namely decreased IENFD and indicates that overexpression of human mutations generates a zebrafish model of SFN (Estacion et al., 2011, Hoeijmakers et al., 2012b, Faber et al., 2012a). Further supporting our findings, the overexpression of the p.(I288M) variant in DRG neurons was proved to induce 20% reduction of neurite length after 3 days in culture (Persson et al., 2013). Conversely, the p.(G856D) mutation did not cause significant effects on neurite length in rodent DRG neurons after 3 days in culture, though a significant reduction was observed after 30 days in culture (Rolyan et al., 2016).

An explanation for the difference between these *in vitro* studies with rodent DRG neurons and our results in zebrafish embryos might be found in the different types of sensory neurons. Zebrafish have at this early developmental stage mainly RB neurons. RB neurons are an early type of sensory neurons that are transiently present and replaced by DRG neurons (Svoboda et al., 2001, Malafoglia et al., 2013). This transition is mediated by the apoptosis of RBs that starts early in development; however, retraction of RB neurites is not reported before 48 hpf (Svoboda et al., 2001). Apoptosis in RB neurons is regulated by the electrical activity of these neurons. A reduction of Na^+-current by pharmacological inhibition (tricaine) or a genetic loss (*mao* mutants) of functional sodium channels significantly reduced apoptosis and resulted in the presence of RB neurons at later stages of development (Svoboda et al., 2001). Since increased Na^+ influx in DRG neurites expressing these mutations have been associated with injurious levels of axonal Ca^{2+} probably mediated by a reverse operating of the Na^+/Ca^{2+} exchanger, we hypothesized that increased levels of Na^+ current produced by the mutant channels could contribute to early apoptosis of RB neurons and thereby a decreased nerve density as observed in our study (Persson et al., 2016, Persson et al., 2013, Estacion et al., 2015). Interestingly, at 48 hpf we did not observe any

differences in the number of apoptotic RB neurons between embryos expressing *SCN9A*-WT and the mutant constructs (Supp. fig. 7). These results indicate that the decreased nerve densities are not caused by an increase of RB neuron death at this developmental stage. However, it could be that the defects arise in earlier developmental stages or that other mechanisms underlie our observations. Furthermore, it is important to note that a clear functional ortholog of human *SCN9A* in teleost species has not been identified to date (Widmark et al., 2011). As $Na_v1.7$ GOF mutations are inherited in an autosomal dominant manner, we have opted for the use of an overexpression model (Faber et al., 2012a). Besides overexpression has the main advantage to test relatively fast the effect of VUS in comparison to the generation of genetic lines which requires raising several generations. Therefore, this approach would allow us to provide rapidly information about the increasing number of VUS.

The second read-out is measured at a later developmental stage (96 hpf), where DRG neurons are gradually taking over the functions of RB neurons (Reyes et al., 2004). At this stage, we observed an increase in temperature-related activity for larvae expressing the p.(I228M) mutation, resembling thermal allodynia observed in patients with this mutation. Remarkably, for the p.(G856D) mutation which is also known to cause thermal allodynia we did not observe an increase in temperature-related activity. These findings suggest that at this stage the p.(I228M) mutant channels had a more pronounced effect on zebrafish DRG neuron functioning. This is further supported by data from DRG culture studies, where the p.(I288M) mutation had at earlier stages an effect on DRG neurite length in comparison to the p.(G856D) mutation (Persson et al., 2013, Rolyan et al., 2016).

There are some caveats to this study. First, we note that Nav1.7 has been reported to be expressed in keratinocytes of mammals (Zhao et al., 2008). The present results do not exclude the possibility that functional Nav1.7 channels were expressed in zebrafish skin cells, in addition to or instead of in sensory neurons. Expression in these skin cells could, in principle, explain the behavioral findings. Furthermore, expression in skin could secondarily affect the pattern of innervation, i.e. IENFD. Even if this is the case, however, it does not detract from our conclusion that expression of GOF Nav1.7 mutant channels can be detected in zebrafish in terms of changes that mimic the morphological and clinical manifestations of SFN. Second, our behavioral read-out demonstrated a clear increase in activity at elevated temperatures for the p.(I228M) mutation, but not for p.(G856D). Whether this reflects

different functional profiles of the two mutations as documented previously (Estacion et al., 2011, Hoeijmakers et al., 2012b) or an experimental issue such as different patterns of expression within the zebrafish background, remains to be determined. Irrespective of this, however, we would note that, for the p.(I228M) mutation, the zebrafish model paralleled the clinical presentation on both a morphological and behavioral basis.

In conclusion, we have successfully expressed two pathogenic *SCN9A* mutations in an *in vivo* zebrafish model. The functional consequences of these substitutions were tested in a newly developed read-out panel based on diagnostic criteria of SFN, which revealed a significant effect on sensory nerve density for both mutations. In addition to this morphological result which parallels the clinical profile of SFN, our observations demonstrated a significant increase in activity at elevated temperatures for the p.(I228M) mutation. Taken together, our results suggest that zebrafish may provide a novel model for assessing the pathogenicity of VUS substitutions identified in molecular diagnostic tests. Given the many advantages of zebrafish as an experimental platform, our data suggest a new model for SFN that could be of interest in studying pathophysiology and for initial screening of potential therapeutic interventions.

Figure legends

Figure 1. Sensory neurite development in the caudal fin of *sensory:GFP* embryos at different timepoints.

Sensory neurite development in the caudal fin of *sensory:GFP* embryos was followed at several stages of development (24, 36, 48, and 56 hpf). Indicated by the red frame is the developmental stage (48 hpf) that was used to study the effect of the pathogenic p.(I228M) and p.(G856D) mutation. Images represent maximal projections of confocal recordings at 20x magnification. Scale bar indicates 100 µm.

Figure 2. Development of a temperature-controlled water compartment.

Panel A. Water reservoir and flow/temperature controller are assembled in two units. The water reservoir unit contains a tank which feeds the water compartment. The controller unit controls flow rate, temperature and water quality (UV sterilization). Panel B. Because two different water reservoirs like depicted in panel A can feed the water compartment it is possible to rapidly increase or cool down the water temperature of the compartment containing a 48-well plate (Top view and side view of the water compartment). Temperatures were measured by the temperature sensor inside the water compartment and the temperature sensor in the well. Panel C. The average temperature change (± SEM) in 6 different test runs after 10 minutes of recording at baseline temperature. Blackline indicates the temperature in the water compartment and the greyline the average of the temperatures measured inside the wells (± SEM).

Figure 3. Diminished temperature response at 96 hpf for homozygous s*cn8aa* loss-of-function (LOF) mutants.

At 96 hpf Zebrafish embryos of the nebula (*scn8aa* LOF) line, placed in a 48 well plate, were after baseline recording exposed to an elevation of water temperature (dotted line indicates water temperature in the wells plotted on the right y-axis). This resulted in a significantly reduced temperature response for homozygous *scn8aa* mutants (grey line) compared to control: *scn8aa* siblings, WT and heterozygous mutant (black line). Each data point represents the mean value (± SEM) of a total of 96 larvae. Significance was tested with an unpaired students T-test (unequal variances). For all data points during the temperature increase, P values indicated a high level of significance (P<0.0001). Activity is presented as changes in pixels and expressed using Arbitrary Units (AU).

Figure 4. Decreased nerve density in zebrafish embryos (48 hpf) expressing mutant human *SCN9A*.

Analysis of maximal projections with the ImageJ particle analyzer revealed in *sensory:GFP* embryos (48 hpf) expressing *SCN9A* p.(I228M) (Black squares) or *SCN9A* p.(G856D) (Black triangles), a significantly decreased nerve density in the tail section, when compared to embryos expressing *SCN9A*-WT (Black circles). Representative maximal projections of each group are depicted in the upper panel. Each data point represents

15

the average GFP% in the caudal fin per zebrafish embryo and consists of the analysis of 5 independent regions. The horizontal line depicts the mean value with SEM. Significance was tested with an unpaired students T-test (unequal variances). ***Indicates for both comparisons a p-value of 0.0005. $n^{SCN9A\text{-}WT}$= 12, $n^{SCN9A\ p.(I228M)}$ 13, $n^{SCN9A\ p.(G856D)}$=7. Image acquisition, at a magnification of 20x, was performed with a confocal microscope (DMI 4000B microscope equipped with a TCS SPE confocal laser scanning module (Leica, Wetzlar, Germany). Scale bar indicates 100μm.

Figure 5. Increased activity at elevated temperatures for larvae (96 hpf) expressing the *SCN9A* p.(I228M) mutation.

At 96 hpf, embryos expressing human (mutant) *SCN9A* were exposed to an elevation of water temperature (dotted line indicates water temperature in the wells plotted on the right y-axis). This resulted in a significantly increased activity at elevated temperatures for larvae expressing the *SCN9A* p.(I228M) mutation (Black line panel A). The maximal activity at the elevated temperatures for the larvae expressing the p.(I228M) mutation is depicted in panel B. Larvae expressing the p.(G856D) mutation (black line panel C) no significant differences were observed. The maximal activity at the elevated temperatures for larvae expressing the p.(G856D) mutation is depicted in panel D. Each data point represents the mean value with SEM. (A,B) $n^{SCN9A\text{-}WT}$=92, $n^{SCN9A\ p.(I228M)}$ 96. (C,D) $n^{SCN9A\text{-}WT}$= 69 , $n^{SCN9A\ p.(G856D)}$= 68. *Significance was tested with an unpaired student's T-test (unequal variances) and was demonstrated for 2 time points, 14 minutes (p value 0.033) and 15 minutes (p value 0.0486) (A). Activity is presented as changes in pixels and expressed in Arbitrary Units (AU).

16

Competing interests

The authors declare no competing or financial interests.

Authors contribution statement

Conceptualization: I.E., J.M.V.; **Methodology** I.E., A.B.C.O., J.M.V.; **Validation**: I.E., J.M.V.; **Formal analysis**: I.E.; **Investigation**: I.E.; **Resources**: H.J.M.S., C.G.F.; **Writing - original draft**: I.E., J.M.V.; **Writing - review & editing**: M.S., A.B.C.O., M.M.G., J.G.J.H., S.G.W., R.L., G.L., I.S.J.M., H.J.M.S., C.G.F., J.M.V.; **Visualization:** I.E.; **Supervision**: J.M.V., H.J.M.S., C.G.F.; **Funding acquisition**: S.G.W., G.L., I.S.J.M., H.J.M.S., C.G.F., J.M.V.

References

AVDESH, A., CHEN, M., MARTIN-IVERSON, M. T., MONDAL, A., ONG, D., RAINEY-SMITH, S., TADDEI, K., LARDELLI, M., GROTH, D. M., VERDILE, G. & MARTINS, R. N. 2012. Regular care and maintenance of a zebrafish (Danio rerio) laboratory: an introduction. *J Vis Exp*, e4196.

BECKER, T. S. & RINKWITZ, S. 2012. Zebrafish as a genomics model for human neurological and polygenic disorders. *Dev Neurobiol,* 72**,** 415-28.

BLACK, J. A., FREZEL, N., DIB-HAJJ, S. D. & WAXMAN, S. G. 2012. Expression of Nav1.7 in DRG neurons extends from peripheral terminals in the skin to central preterminal branches and terminals in the dorsal horn. *Mol Pain,* 8**,** 82.

CAZZATO, D. & LAURIA, G. 2017. Small fibre neuropathy. *Curr Opin Neurol,* 30**,** 490-499.

COX, J. J., SHEYNIN, J., SHORER, Z., REIMANN, F., NICHOLAS, A. K., ZUBOVIC, L., BARALLE, M., WRAIGE, E., MANOR, E., LEVY, J., WOODS, C. G. & PARVARI, R. 2010. Congenital insensitivity to pain: novel SCN9A missense and in-frame deletion mutations. *Hum Mutat,* 31**,** E1670-86.

CURTRIGHT, A., ROSSER, M., GOH, S., KEOWN, B., WAGNER, E., SHARIFI, J., RAIBLE, D. W. & DHAKA, A. 2015. Modeling nociception in zebrafish: a way forward for unbiased analgesic discovery. *PLoS One,* 10**,** e0116766.

DE GREEF, B. T. A., HOEIJMAKERS, J. G. J., GORISSEN-BROUWERS, C. M. L., GEERTS, M., FABER, C. G. & MERKIES, I. S. J. 2017. Associated conditions in small fiber neuropathy - a large cohort study and review of the literature. *Eur J Neurol*.

DEVIGILI, G., TUGNOLI, V., PENZA, P., CAMOZZI, F., LOMBARDI, R., MELLI, G., BROGLIO, L., GRANIERI, E. & LAURIA, G. 2008. The diagnostic criteria for small fibre neuropathy: from symptoms to neuropathology. *Brain,* 131**,** 1912-25.

ESTACION, M., HAN, C., CHOI, J. S., HOEIJMAKERS, J. G., LAURIA, G., DRENTH, J. P., GERRITS, M. M., DIB-HAJJ, S. D., FABER, C. G., MERKIES, I. S. & WAXMAN, S. G. 2011. Intra- and interfamily phenotypic diversity in pain syndromes associated with a gain-of-function variant of NaV1.7. *Mol Pain,* 7**,** 92.

ESTACION, M., VOHRA, B. P., LIU, S., HOEIJMAKERS, J., FABER, C. G., MERKIES, I. S., LAURIA, G., BLACK, J. A. & WAXMAN, S. G. 2015. Ca2+ toxicity due to reverse Na+/Ca2+ exchange contributes to degeneration of neurites of DRG neurons induced by a neuropathy-associated Nav1.7 mutation. *J Neurophysiol,* 114**,** 1554-64.

FABER, C. G., HOEIJMAKERS, J. G., AHN, H. S., CHENG, X., HAN, C., CHOI, J. S., ESTACION, M., LAURIA, G., VANHOUTTE, E. K., GERRITS, M. M., DIB-HAJJ, S., DRENTH, J. P., WAXMAN, S. G. & MERKIES, I. S. 2012a. Gain of function Nanu1.7 mutations in idiopathic small fiber neuropathy. *Ann Neurol,* 71**,** 26-39.

FABER, C. G., LAURIA, G., MERKIES, I. S., CHENG, X., HAN, C., AHN, H. S., PERSSON, A. K., HOEIJMAKERS, J. G., GERRITS, M. M., PIERRO, T., LOMBARDI, R., KAPETIS, D., DIB-HAJJ, S. D. & WAXMAN, S. G. 2012b. Gain-of-function Nav1.8 mutations in painful neuropathy. *Proc Natl Acad Sci U S A,* 109**,** 19444-9.

GAU, P., POON, J., UFRET-VINCENTY, C., SNELSON, C. D., GORDON, S. E., RAIBLE, D. W. & DHAKA, A. 2013. The zebrafish ortholog of TRPV1 is required for heat-induced locomotion. *J Neurosci,* 33**,** 5249-60.

HAN, C., YANG, Y., DE GREEF, B. T., HOEIJMAKERS, J. G., GERRITS, M. M., VERHAMME, C., QU, J., LAURIA, G., MERKIES, I. S., FABER, C. G., DIB-HAJJ, S. D. & WAXMAN, S. G. 2015. The Domain II S4-S5 Linker in Nav1.9: A Missense Mutation Enhances Activation, Impairs Fast Inactivation, and Produces Human Painful Neuropathy. *Neuromolecular Med,* 17**,** 158-69.

HO, C. & O'LEARY, M. E. 2011. Single-cell analysis of sodium channel expression in dorsal root ganglion neurons. *Mol Cell Neurosci,* 46**,** 159-66.

HOEIJMAKERS, J. G., FABER, C. G., LAURIA, G., MERKIES, I. S. & WAXMAN, S. G. 2012a. Small-fibre neuropathies--advances in diagnosis, pathophysiology and management. *Nat Rev Neurol,* 8**,** 369-79.

HOEIJMAKERS, J. G., HAN, C., MERKIES, I. S., MACALA, L. J., LAURIA, G., GERRITS, M. M., DIB-HAJJ, S. D., FABER, C. G. & WAXMAN, S. G. 2012b. Small nerve fibres, small hands and small feet: a new syndrome of pain, dysautonomia and acromesomelia in a kindred with a novel NaV1.7 mutation. *Brain,* 135**,** 345-58.

HOEIJMAKERS, J. G. J. 2014. *Small fiber neuropathy and sodium channels: A paradigm shift.* PhD, MD PhD, Maastricht University.

LISTER, J. A., ROBERTSON, C. P., LEPAGE, T., JOHNSON, S. L. & RAIBLE, D. W. 1999. nacre encodes a zebrafish microphthalmia-related protein that regulates neural-crest-derived pigment cell fate. *Development,* 126**,** 3757-67.

LOW, S. E., ZHOU, W., CHOONG, I., SAINT-AMANT, L., SPRAGUE, S. M., HIRATA, H., CUI, W. W., HUME, R. I. & KUWADA, J. Y. 2010. Na(v)1.6a is required for normal activation of motor circuits normally excited by tactile stimulation. *Dev Neurobiol,* 70**,** 508-22.

MALAFOGLIA, V., BRYANT, B., RAFFAELI, W., GIORDANO, A. & BELLIPANNI, G. 2013. The zebrafish as a model for nociception studies. *J Cell Physiol,* 228**,** 1956-66.

MARBAN, E., YAMAGISHI, T. & TOMASELLI, G. F. 1998. Structure and function of voltage-gated sodium channels. *J Physiol,* 508 (Pt 3)**,** 647-57.

NOVAK, A. E., TAYLOR, A. D., PINEDA, R. H., LASDA, E. L., WRIGHT, M. A. & RIBERA, A. B. 2006. Embryonic and larval expression of zebrafish voltage-gated sodium channel alpha-subunit genes. *Dev Dyn,* 235**,** 1962-73.

NUSSLEIN-VOLHARD, C. & DAHM, R. 2002. *Zebrafish* Oxford UK.

O'BRIEN, G. S., RIEGER, S., WANG, F., SMOLEN, G. A., GONZALEZ, R. E., BUCHANAN, J. & SAGASTI, A. 2012. Coordinate development of skin cells and cutaneous sensory axons in zebrafish. *J Comp Neurol,* 520**,** 816-31.

PERSSON, A. K., HOEIJMAKERS, J. G., ESTACION, M., BLACK, J. A. & WAXMAN, S. G. 2016. Sodium Channels, Mitochondria, and Axonal Degeneration in Peripheral Neuropathy. *Trends Mol Med,* 22**,** 377-90.

PERSSON, A. K., LIU, S., FABER, C. G., MERKIES, I. S., BLACK, J. A. & WAXMAN, S. G. 2013. Neuropathy-associated Nav1.7 variant I228M impairs integrity of dorsal root ganglion neuron axons. *Ann Neurol,* 73**,** 140-5.

PINEDA, R. H., HEISER, R. A. & RIBERA, A. B. 2005. Developmental, molecular, and genetic dissection of INa in vivo in embryonic zebrafish sensory neurons. *J Neurophysiol,* 93**,** 3582-93.

PROBER, D. A., ZIMMERMAN, S., MYERS, B. R., MCDERMOTT, B. M., JR., KIM, S. H., CARON, S., RIHEL, J., SOLNICA-KREZEL, L., JULIUS, D., HUDSPETH, A. J. & SCHIER, A. F. 2008. Zebrafish TRPA1 channels are required for chemosensation but not for thermosensation or mechanosensory hair cell function. *J Neurosci,* 28**,** 10102-10.

REYES, R., HAENDEL, M., GRANT, D., MELANCON, E. & EISEN, J. S. 2004. Slow degeneration of zebrafish Rohon-Beard neurons during programmed cell death. *Dev Dyn,* 229**,** 30-41.

ROLYAN, H., LIU, S., HOEIJMAKERS, J. G., FABER, C. G., MERKIES, I. S., LAURIA, G., BLACK, J. A. & WAXMAN, S. G. 2016. A painful neuropathy-associated Nav1.7 mutant leads to time-

dependent degeneration of small-diameter axons associated with intracellular Ca2+ dysregulation and decrease in ATP levels. *Mol Pain,* 12.

SHIELDS, S. D., AHN, H. S., YANG, Y., HAN, C., SEAL, R. P., WOOD, J. N., WAXMAN, S. G. & DIB-HAJJ, S. D. 2012. Nav1.8 expression is not restricted to nociceptors in mouse peripheral nervous system. *Pain,* 153**,** 2017-30.

SVOBODA, K. R., LINARES, A. E. & RIBERA, A. B. 2001. Activity regulates programmed cell death of zebrafish Rohon-Beard neurons. *Development,* 128**,** 3511-20.

TAYLOR, J. C., DEWBERRY, L. S., TOTSCH, S. K., YESSICK, L. R., DEBERRY, J. J., WATTS, S. A. & SORGE, R. E. 2017. A novel zebrafish-based model of nociception. *Physiol Behav,* 174**,** 83-88.

TESFAYE, S., BOULTON, A. J., DYCK, P. J., FREEMAN, R., HOROWITZ, M., KEMPLER, P., LAURIA, G., MALIK, R. A., SPALLONE, V., VINIK, A., BERNARDI, L., VALENSI, P. & TORONTO DIABETIC NEUROPATHY EXPERT, G. 2010. Diabetic neuropathies: update on definitions, diagnostic criteria, estimation of severity, and treatments. *Diabetes Care,* 33**,** 2285-93.

WAXMAN, S. G., MERKIES, I. S., GERRITS, M. M., DIB-HAJJ, S. D., LAURIA, G., COX, J. J., WOOD, J. N., WOODS, C. G., DRENTH, J. P. & FABER, C. G. 2014. Sodium channel genes in pain-related disorders: phenotype-genotype associations and recommendations for clinical use. *Lancet Neurol,* 13**,** 1152-60.

WIDMARK, J., SUNDSTROM, G., OCAMPO DAZA, D. & LARHAMMAR, D. 2011. Differential evolution of voltage-gated sodium channels in tetrapods and teleost fishes. *Mol Biol Evol,* 28**,** 859-71.

WOOD, J. N. & BAKER, M. 2001. Voltage-gated sodium channels. *Curr Opin Pharmacol,* 1**,** 17-21.

WRIGHT, M. A., MO, W., NICOLSON, T. & RIBERA, A. B. 2010. In vivo evidence for transdifferentiation of peripheral neurons. *Development,* 137**,** 3047-56.

ZHAO, P., BARR, T. P., HOU, Q., DIB-HAJJ, S. D., BLACK, J. A., ALBRECHT, P. J., PETERSEN, K., EISENBERG, E., WYMER, J. P., RICE, F. L. & WAXMAN, S. G. 2008. Voltage-gated sodium channel expression in rat and human epidermal keratinocytes: evidence for a role in pain. *Pain,* 139**,** 90-105.

Highlights

- Set up of two read-outs reflecting Small-fiber neuropathy in zebrafish.

- Expression of mutant *SCN9A* provides a model for Small-fiber neuropathy in zebrafish.

- Development of a temperature-controlled water compartment.